

give rise to values of  $\mu_{zz}'$  and  $\mu_{zz}''$  of the order of 2-5 and  $\kappa \sim 1$ . If now we consider the higher frequency ranges, for example frequencies of the order of 35 Gc/s, we may select long or short toroids of ferrites with  $4000 < 4\pi M_s < 6000$  Gs for operation well above resonance in the range  $2.0 < \sigma < 3.3$ . Such materials [5] are NiZn-ferrite ( $4\pi M_s = 4000$  Gs), Mn-ferrite ( $4\pi M_s = 5200$  Gs) and Fe-ferrite ( $4\pi M_s = 6000$  Gs).

Finally, we briefly discuss the application of these results to low-power latching resonance isolators, or digital amplitude modulators. The longer toroids ( $N_s \sim 0.9$ ) exhibit a resonance at  $\omega/\omega_m \sim 0.25$ . This means that isolators could be constructed at frequencies around 0.75 Gc/s, 1.5 Gc/s, and 3 Gc/s using materials with values of  $4\pi M_s$  of the order of 1070, 2140, and 4280 Gs, respectively. However, a greater range of materials and frequencies becomes available if we choose short toroids ( $N_s \sim 0.5$ ). In these, resonance occurs at  $\omega/\omega_m \sim 0.5$ , and consequently, isolators at frequencies of 0.75, 1.5, 3.0, 6.0, 10.0 Gc/s can be made using materials with values of  $4\pi M_s$  of the order of 535, 1070, 2140, 4280, 7150 Gs. Once a suitable material is chosen for a frequency range, a toroid could be tuned to resonance at a selected frequency by adjusting the length, and a broader bandwidth may be possible using several toroids of different lengths.

Finally, it should be noted that the effects of anisotropy and the unsaturated regions of the toroid have not been taken into account. These factors will broaden the linewidth, so that in practice it will not be possible to work a phase shifter as near to resonance as the theory predicts. Also, it is to be expected that the predicted values of resonant frequencies will in practice be modified, if the vertical walls of the toroid are in close proximity and the height of the toroid window is appreciably different from the waveguide height. This theory will therefore apply most closely to a structure in which the vertical walls of the toroid are widely spaced and the magnetic circuit is completed outside the waveguide.

To summarize: The effect on the permeability tensor of shape and material linewidth has been computed for four sizes of toroid and two values of normalized linewidth. It has been shown that to avoid losses with values of  $\Delta H/2(4\pi M_s) \sim 0.015$ , corresponding to the commercially available polycrystalline garnets, short toroids ( $0.7 < N_s < 0.9$ ) may be used above or below resonance, and long toroids ( $N_s > 0.9$ ) only above resonance. With broader linewidths,  $\Delta H/2(4\pi M_s) \sim 0.10$ , losses can be avoided only by working above resonance whatever the shape of toroid. The way in which recently reported latching phase shifters agree with these generalizations has been discussed. On the basis of these computations suitable materials and shapes for operation in other frequency bands have been suggested. Also, materials and shapes for digital modulators, i.e., latching resonance isolators, have been discussed briefly.

L. E. DAVIS  
Dept. of Elec. Engrg.  
Rice University  
Houston, Tex.

# REFERENCES

- [1] K. J. Button and B. Lax, *Microwave Ferrites and Ferromagnetics*, New York: McGraw-Hill, 1962, p. 159, equations (4)-(29) and p. 195, equations (4)-(79). (Read  $(N_x + N_y)$  for  $(N_s - N_y)$  in the denominators.)
- [2] D. R. Taft and L. R. Hodges "Square-loop garnet materials for digital phase-shifter applications" *J. Appl. Phys.*, vol. 36, no. 3, pt. 2, p. 1263, March 1965.
- [3] L. R. Whicker and R. R. Jones, "A digital latching ferrite strip transmission line phase shifter; Taft, et al., "Ferrite digital phase shifters; Landry and Passaro, "A four-bit latching ferrite switch," all three papers presented at 1965 G-MTT Symposium, Clearwater, Fla.
- [4] E. Schlömann, "Theoretical analysis of twin slab phase shifters in rectangular waveguides," presented at 1965 G-MTT Symposium, Clearwater, Fla.
- [5] K. J. Button and B. Lax, *op. cit.* [1], pp. 163 and 703-705.

The components of a radial TEM wave are

$$E_r(kr) = AJ_0(kr) + BN_0(kr) \\ -j\eta H_\phi(kr) = AJ_1(kr) + BN_1(kr). \quad (1)$$

$A$  and  $B$  are complex quantities and  $k = 2\pi/\lambda = 2\pi f/c$ .

For a radial line short-circuited at the edge  $r=R$ ,  $E_r(kR) = 0$  and, hence,  $A = -B N_0(kR)/J_0(kR)$ . The input admittance becomes

$$Y_{in}(r) = -\frac{2\pi r H_\phi(kr)}{d \cdot E_r(kr)} \\ = -\frac{j}{\eta} \frac{kr}{d/\lambda} \frac{F_1(kr)}{F_0(kr)} \quad (2)$$

where

$$F_0(kr) = J_0(kr)N_0(kR) - N_0(kr)J_0(kR) \\ F_1(kr) = J_1(kr)N_0(kR) - N_1(kr)J_0(kR). \quad (3)$$

In antiresonance  $f = f_0$  ( $k = k_0$ ) is  $F_1(k_0 r) = 0$ . The slope parameter for the input admittance is then as can be seen

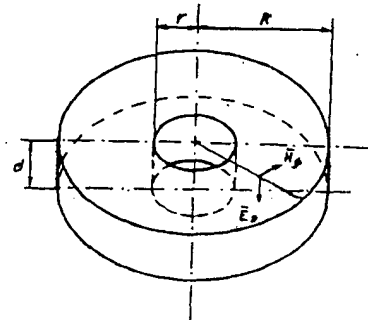


Fig. 1. The radial resonator.

# Slope Parameter and Q of Radial Resonators

A radial resonator, Fig. 1, has proved useful, e.g., in filter constructions of coaxial parametric amplifiers [1]. As a band rejection filter in a coaxial line, the radial resonator lies in antiresonance. Thus, it opens up the outer conductor efficiently, and power at this frequency band is reflected back. For filter design purposes, it may be useful to know what are the slope parameter and the  $Q$  of the resonator. In the following, a formula for the characteristic impedance of the equivalent uniform TEM short-circuited  $\lambda/4$ -resonator is derived, whose slope factor is the same as that of the radial antiresonant line. In design work, the radial line can be replaced by this  $\lambda/4$ -line around the center frequency. A formula for the  $Q$  of the resonator is also derived.

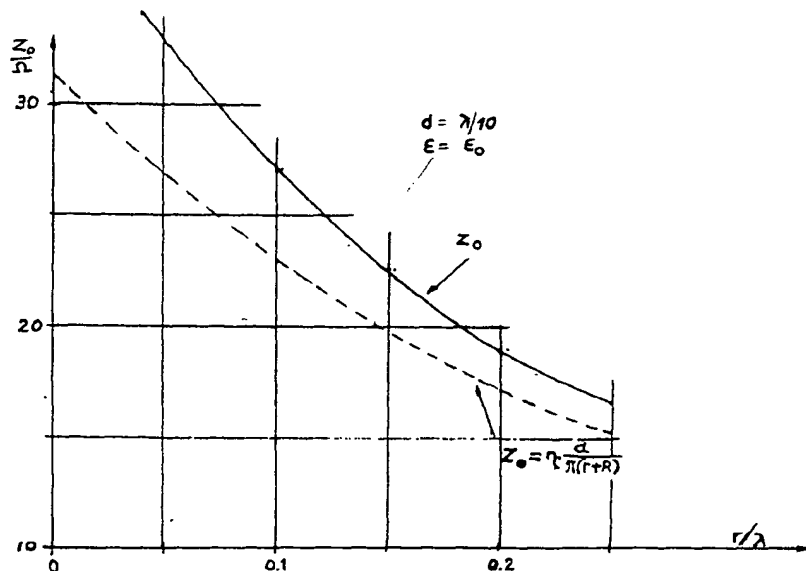


Fig. 2. The  $Z_0$  of a uniform TEM short-circuited transmission line whose slope parameter = that of the radial resonator.

Manuscript received October 5, 1965.

$$\left. \frac{dY_{in}}{df} \right|_{f_0} = \left. \frac{dY_{in}}{dk} \right|_{k_0} \frac{k_0}{f_0} = \frac{j}{\eta} \frac{k_0^2 r^2}{f_0(d/\lambda_0)} \left[ \frac{RG_1(k_0 r)}{rF_0(k_0 r)} - 1 \right] \quad (4)$$

where

$$G_1(kr) = J_1(kr)N_1(kR) - N_1(kr)J_1(kR). \quad (5)$$

For a uniform  $\lambda/4$ -transmission line

$$\left. \frac{dY_{in}}{df} \right|_{f_0} = j \frac{\pi}{2} \frac{1}{Z_0 f_0} \quad (6)$$

where  $Z_0$  is the characteristic impedance of the line. By setting the right-hand sides of (4) and (6) equal, the equivalent  $Z_0$  of the radial antiresonant line may be solved. It becomes

$$Z_0 = \frac{\eta}{8\pi} \frac{d/\lambda_0}{(r/\lambda_0)^2} \frac{1}{\left[ \frac{R}{r} \frac{G_1(k_0 r)}{F_0(k_0 r)} - 1 \right]} \quad (7)$$

In Fig. 2, the dependence of  $Z_0$  on  $r/\lambda_0$  is plotted in the case of the lowest antiresonance. In the same diagram, the characteristic impedance of a strip line with a strip width equal to the mean circumference of the radial line is also presented for comparison. In both cases, a distance  $d$  of  $\lambda/10$  and air filling is assumed but the results may easily be calculated for other distances and fillings, by multiplying with  $d/0.1\lambda$  and dividing with  $\sqrt{\epsilon_r}$ , as is seen from (7). For solving the equation  $F_1(k_0 r) = 0$ , we refer to a diagram in [2]. The  $Q$  of the resonator, calculated by definition (8), leads to (9).

$$Q = \frac{\omega_0 \cdot \text{energy stored in the resonator}}{\text{average power loss in the walls}} \quad (8)$$

$$Q = \frac{\omega_0 \eta^2 d}{R_s} \frac{\int_0^R r F_0^2(k_0 r) dr}{\left[ 2 \int_0^R r F_1^2(k_0 r) dr + R d F_1^2(k_0 R) \right]} \quad (9)$$

$R_s$  is the surface resistance of the resonator material at the given frequency. For a linear combination  $F_p$  of Bessel and Neumann functions of order  $p$

$$\int_0^R r F_p^2(kr) dr = \frac{r^2}{2} [F_p^2(kr) - F_{p-1}(kr)F_{p+1}(kr)] \quad (10)$$

is valid. Noting that  $F_1(k_0 r) = 0$  and  $F_0(k_0 R) = 0$  we see that

$$\int_0^R r F_1^2(k_0 r) dr = \int_0^R r F_2^2(k_0 r) dr$$

$$\left[ = \frac{1}{2} R^2 F_1^2(k_0 R) - r^2 F_0^2(k_0 r) \right], \quad (11)$$

thus giving the value of  $Q$ :

$$Q = \frac{\omega_0 \eta^2}{2R_s} \frac{R^2 F_1^2(k_0 R) - r^2 F_0^2(k_0 r)}{\left[ R(R+d)F_1^2(k_0 R) - r^2 F_0^2(k_0 r) \right]}. \quad (12)$$

The factor in brackets is practically a constant depending on values of  $d$  only and can be approximated with  $R/(R+d)$ , the error being within a few percent. This is the case

of the cylindrical resonator ([3], p. 428) and can directly be deduced from (12) by omitting the terms with  $r$ .

ISMO V. LINDELL  
Radio and Electronics Lab.  
Dept. of Elec. Engrg.  
Institute of Technology  
Helsinki, Finland

#### REFERENCES

- [1] B. C. De Loach, Jr., "Radial-line coaxial filters in the microwave region," *IEEE Trans. on Microwave Theory and Techniques*, vol. MTT-11 pp. 50-55, January 1963.
- [2] *The Microwave Engineers' Handbook 1965*. New York: Horizon House-Microwave Inc., p. 54.
- [3] S. Ramo and J. R. Whinnery, *Fields and Waves in Modern Radio*, 2nd ed., New York: Wiley, 1953.

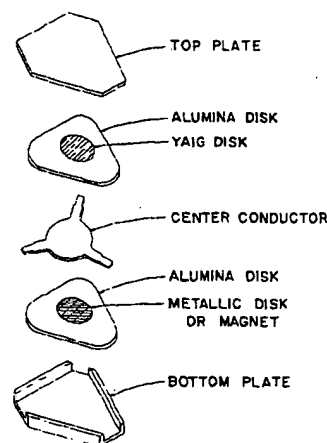


Fig. 1. Exploded view of a three-port circulator with metallic short between the center conductor and ground.

#### A Novel Strip-Line Circulator

A circulator with strip-line inputs has been developed which incorporates a single disk of yttrium aluminum iron garnet (YAIG) on one side of the center conductor and a large, metallic short circuit on the other side. The short circuit can be the magnet necessary to bias the garnet to the optimum field for broadband circulation. The basic design is shown in Fig. 1. The center conductor junction is round with alumina loaded quarter-wave transformer coupling to the 50- $\Omega$  input lines. Compared to a standard circulator with two YAIG disks operating in the same frequency range, the center conductor diameter is somewhat larger and the transformers of somewhat lower impedance. The metallic disk is smaller than the center conductor diameter and is one of the factors which determine the resonant frequency of the junction. The performance of a typical unit is plotted in Fig. 2. This isolation characteristic is double humped and ranges from 30 to 40 dB across a 13.7 percent frequency band. The insertion loss is 0.2 dB across the same band.

In order to understand the modal configuration which allows circulation to exist in this design, a completely air loaded two-port transmission structure was built as shown in Fig. 3. The junction diameter was kept the same as the circulator. A large number of small diameter probing holes were included in the walls and the fields were examined at the resonant frequencies of the structure. The lowest mode occurs at 1.48 GHz. The magnetic field lines are concentric circles about the axis of symmetry. The maximum "h" field intensity occurs around the short-circuiting disk and continuously decreases to a minimum at the center of the opposite side of the structure. This mode, by itself, cannot be used for circulation. In a three-port structure, with the ferrite and alumina in place, the mode would occur at approximately one third the frequency of the circulator. The mode of interest for circulation was found at 4.92 GHz and has the field pattern of Fig. 4. This pattern is similar to the dipolar mode

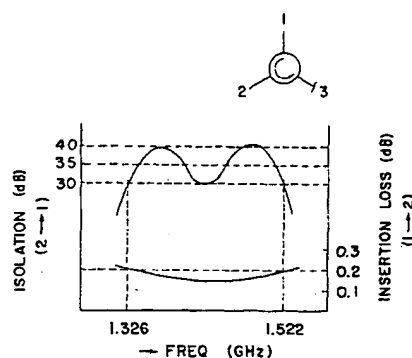


Fig. 2. Isolation and insertion loss characteristics of the circulator.

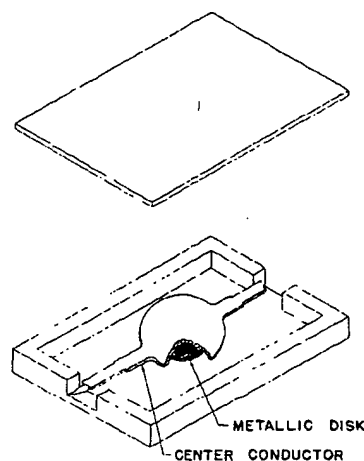


Fig. 3. Two-port air loaded resonant structure.

described by Fay and Comstock.<sup>1</sup> In a symmetrical three-port configuration with a magnetized ferrite disk in the junction region, this pattern can be rotated in the proper manner for circulation.

It is also possible to extend this matching

<sup>1</sup> C. E. Fay and R. L. Comstock, "Operation of the ferrite junction circulator," *IEEE Trans. on Microwave Theory and Techniques*, vol. MTT-13, pp. 15-27 January 1965.